Continuous Monitoring and Mechanism of Electrostatic Charge of Powder in Fluidized Bed Process

Satoru WATANO,* Teruo SUZUKI, Toshinari TAIRA, and Kei MIYANAMI

Department of Chemical Engineering, Osaka Prefecture University, 1–1 Gakuen-cho, Sakai, Osaka 599–8531, Japan.
Received May 14, 1998; accepted June 5, 1998

In a previous paper (Watano *et al.*, *J. Soc. Powder Technol. Jpn*, 34, 778, 1997), we developed a novel system which could continuously monitor the electrostatic field strength of powder in a fluidized bed process. This paper reports further study related to the electrostatic characteristics of powder. Two novel achievements are described; one is an improvement of the reliability and accuracy of the sensor, and the other is the mechanism and characteristics of the electrostatic charge for different kinds of powder materials. First, the structure of the sensor extremity has been improved to remove the troubles encountered in the previous sensor. By using a double-walled cylinder, the sensor is devised to tolerate severe vibration, high purge air flow and particle sticking. By increasing the sensitivity, the accuracy of measurement can be increased by approximately five times that of the previous sensor. Secondly, the relationship between electrostatic field strength and the electrical charge of the particles has been investigated using various kinds of powder materials. The sensor shows a good linearity between two measurements, proving that the electrostatic characteristics of charged particles could be monitored correctly *via* the electrostatic field strength. The performance of the system has been confirmed in the fluidized bed granulation/drying processes using different kinds of particles. The mechanism of the electrostatic charge for different kinds of powdered materials are also discussed.

Key words electrostatic; sensor; electrostatic field strength; electrical charge; fluidized bed process

Recently, electrostatic hazards and interference have become a serious problem in powder handling processes.[1,2] Especially, in the processes of grinding, pneumatic transportation, storage, and fluidized bed drying, a spark discharge is frequently observed in the suspending powder phase and at the surface of the accumulated powder bed, which sometimes induces explosion and fire. Therefore, a continuous and quantitative system of measuring electrostatic charges is required to prevent these hazards beforehand.

Up to this time, a Faraday cage[3,4] has been well used to statically investigate the electrostatic characteristics of charged particles, however, it cannot be used correctly and continuously in powder handling processes, because of its insufficient sampling system. A surface electrical potential sensor with a vibrating electrode[5,6] has also been developed and applied for detecting the surface potential of a flat sheet of paper and nylon film.[7] However, this sensor requires calibration of the distance between sensor and object,[8] and it cannot be used for powder handling processes where powders randomly move.

In order to meet the requirement for the continuous monitoring of electrostatics, we have developed an electrostatic detecting system,[9] based on the principle of electrostatic field strength, with an air purge unit to continuously detect electrostatics in powder handling process. However, the sensor was affected awfully by purge air and vibration. Detailed investigation of the mechanisms of electrostatic charge has not yet been done.

In this study, we have tried to improve the structure of the sensor to remove the disadvantageous points encountered in the previous sensor. By using this newly improved sensor, the relationship between electrostatic field strength and the electrical charge of the particles was then investigated using various powdered materials. The performance of the system has been confirmed in the fluidized bed granulation/drying processes using different kinds of powders; the mechanism and characteristics of the electrostatic charge are also discussed.

Detecting Principle of Electrostatic Field Strength Basically, our sensor[9] adopts a technique to detect alternating voltage which is induced at an electrode by periodically chopping the electrostatic field.

If we assume that the chopping cycle is defined as ω (=500 Hz), the area of electrode in which electrostatic field flows is S_0, and the area of electrode which changes periodically due to the electrode vibrating is S_1, then the effective area of the electrode S can easily be estimated as follows:

$$S=S_0+S_1 \sin \omega t \tag{1}$$

An electrical charge q induced by the periodical change in the electrostatic field is calculated by the following Gauss' s law,

$$q=E_0 S \varepsilon_0 \tag{2}$$

where E_0 and ε_0 show the electrostatic field strength and an air dielectric constant, respectively.

Therefore, a current I_s running through an electric resistance R_s connected between electrode and ground is

$$\begin{aligned} I_s &= \mathrm{d}q/\mathrm{d}t \\ &= E_0 \varepsilon_0 \omega S_1 \cos \omega t \end{aligned} \tag{3}$$

The voltage of the electric resistance V_s is thus:

$$\begin{aligned} V_s &= R_s I_s \\ &= R_s E_0 \varepsilon_0 \omega S_1 \cos \omega t \end{aligned} \tag{4}$$

Finally, it is possible to detect the electrostatic field strength E_0 by measuring the voltage V_s between the electric resistance.

It is noteworthy that in the case of measuring an objective surface voltage, electrostatic field strength must be multiplied by the distance d between the object and the electrode.

* To whom correspondence should be addressed.

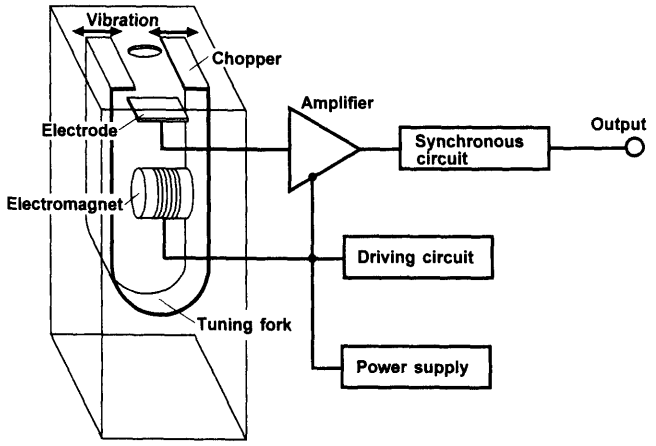

Fig. 1. Schematic Diagram of Sensor

$$V_0=E_0\times d \tag{5}$$

However, in powder handling processes, it is impossible to measure the distance between particles and electrode because particles are moving very fast. So, it is easily understood that the current technique to measure the objective surface voltage to evaluate electrostatic characteristics is not adequate.[6]

In this study, we have focused on the electrostatic field strength to evaluate the electrostatic characteristics because there is no need to measure the distance.

Experimental

Electrostatic Field Sensor Figure 1 shows a schematic diagram of the sensor extremity. This sensor was designed to miniaturize as small as possible (W7×D7×H50 mm). However, it was devised to avoid a decrease in sensor sensibility due to the sensor's miniaturization by amplifying and transmitting the signal with a high *S/N* ratio. Practically, a driving gear composed of a tuning fork and an electric magnet was used. Also, an operational amplifier was used to amplify the signal. By increasing the sensitivity, the accuracy of measurement can be increased by approximately five times that of the previous sensor.

As described previously,[9] our sensor was influenced especially by a purge air flow. This was because the purge air was introduced inside the sensor and the vibration frequency of the tuning fork was affected by the air flow. As shown in Fig.1, the newly developed sensor did not use any purge air going through the sensor.

Figure 2 illustrates the sensor extremity. This newly developed sensor was setup in a double-walled cylinder, and the purge air was blown inside of each cylinder. Powder could not reach to the sensor extremity, and the effect of purge air flow could be neglected. Shock absorbing rubber was placed at an attachment which connected the sensor and fluidized bed wall, in order to remove the effect of vibration. The double-walled cylinder also helped to avoid transmitting vibration to the sensor.

Measurement of Electrical Charge Figure 3 indicates a system used to measure the electrical charge of particles. A Faraday cage composed of an isolated inner cylindrical metal case and an outer cylindrical metal case (electrostatic capacity: C_f, it can be treated as a condenser) for shielding. In the case of measuring the electrical charge of particles, a voltage meter (electrostatic capacity: C_{in}) and a condenser (electrostatic capacity: C_p) were connected between the inner and the outer case. Since the electrostatic capacity, C_p, was basically selected to be much larger than the capacities of the metal case and the voltage meter, the following relationship was obtained:

$$Q=(C_p+C_f+C_{in})V\fallingdotseq C_pV \quad (C_p\gg\gg C_f, C_{in}) \tag{6}$$

The correlation between the electrostatic field strength and the charge of the particles could be measured as follows:

Particles having been shaken in a plastic cylinder for 10 min were fed into the inner case of the Faraday cage. The electrostatic field strength of the particles was measured by the developed system with the distance between the sensor and particles being 5 mm. Simultaneously, the electrical charge of the particles was measured by measuring the electrostatic capacity of the condenser.

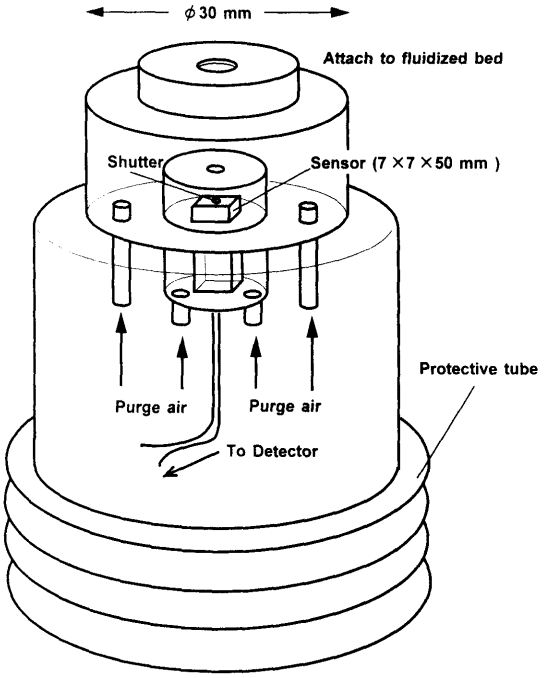

Fig. 2. Schematic Diagram of Sensor Extremity

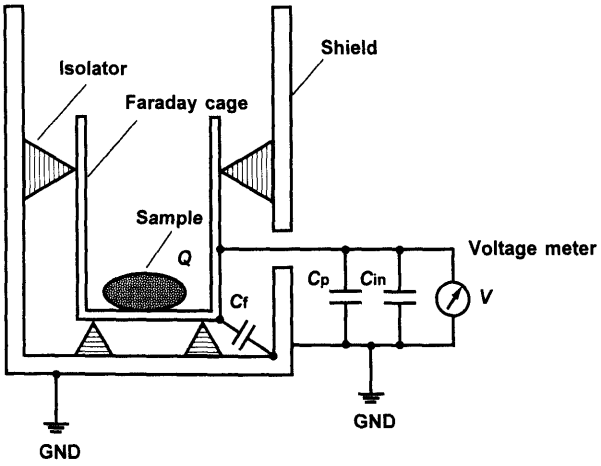

Fig. 3. System Used to Measure Electrical Charge of Particles

Table 1. List of Powder Samples Used

Powder samples	Mass median diameter [μm]	True density [kg/m^3]
Lactose[a]	104	1589
Corn starch[b]	21	1587
Crystalline cellulose[c]	76	1484
Acetaminophen[d]	78	1320
Hydroxypropylcellulose[e]	21	1272

a) Pharmatose 200 M, DMW. *b*) Corn Starch W, Nippon Shokuhin Kakou Co., Ltd. *c*) PH-101, Asahi Chemical Industry Co., Ltd. *d*) Yamamoto Chemical Co., Ltd. *e*) HPC EF-P, Shin-Etsu Chemical Co., Ltd.

Fluidized Bed Figure 4 is a schematic diagram of the fluidized bed used for the experiments. A tapered fluidized bed with an agitator blade[10,11] (NQ-160, Fuji Paudal Co., Ltd.) was used. This fluidized bed consisted of two parts: a lower cylindrical vessel (0.160 m in diameter, 0.160 m in depth) and an upper cone vessel tapered 15 degrees (0.80 m in height), both made of stainless steel. The agitator blade turned on a central axis was installed at the bottom of the cylindrical vessel to impart a tumbling and circulating motion on the granules. Under the blade, a slit plate was stationed for the distribution of fluidizing air. It composed of five circular plates of different diame-

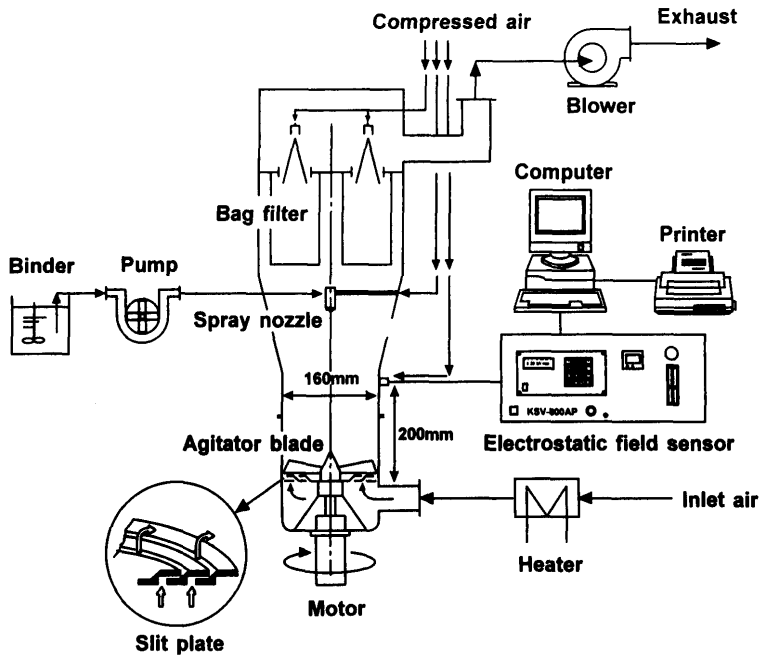

Fig. 4. Schematic Diagram of Fluidized Bed Used

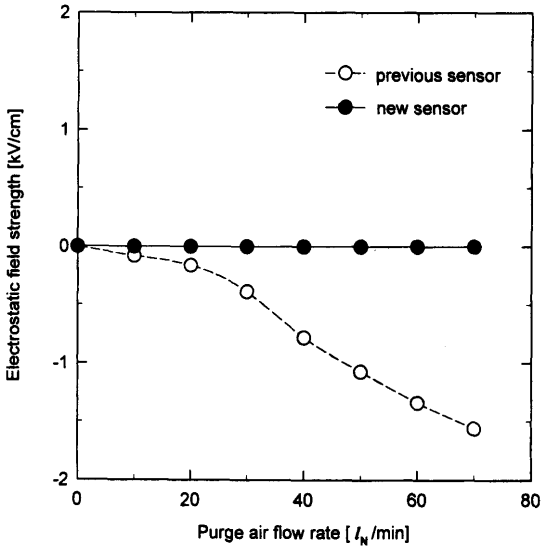

Fig. 5. Effect of Purge Air Flow Rate on the Accuracy of Measurement

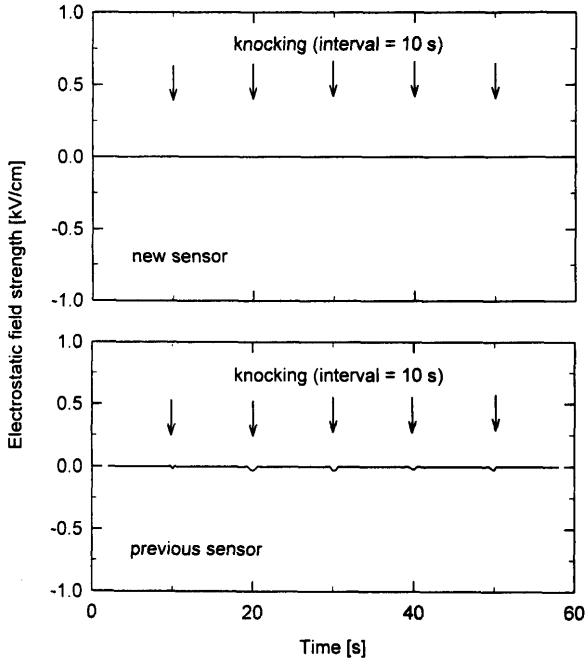

Fig. 6. Effect of Vibration on the Accuracy of Measurement

ters superimposed 0.5 mm apart. Heated air needed for particle fluidization and drying was blown from the slits located between each plate, creating a circulating flow. The electrostatic sensor was connected at the wall of the upper cone vessel (200 mm from the bottom slit plate).

Powder Samples Table 1 lists properties of powder samples used. In this study, pharmaceutical powder of lactose, corn starch, crystalline cellulose, acetaminophen and hydroxypropylcellose were used. Granulated spherical particles made of crystalline cellulose, of which the median diameters were 300 μm (CP-203^R, Asahi Chemical Industry Co., Ltd.), 400 μm (CP-305^R) and 500 μm (CP-507^R) were also used.

Results and Discussion

Performance of the New Sensor Figure 5 shows the effect of purge air flow rate on the accuracy of measurement. The previous sensor showed that electrostatic field strength decreased with an increase in purge air flow rate. This was because the vibrating frequency of the tuning fork inside the sensor was affected by the air flow. However, the new improved sensor indicated no effect of purge air flow. Due to the double-walled cylinder, the purge air touched neither the electrode nor the tuning fork at all.

Figure 6 illustrates the effect of vibration by a knocker (K-30, Seishin Co. Ltd.) used to remove powder adhesion on the wall. For the new sensor, there was no effect of knocking, while the previous sensor received the effect. It seems that the shock absorbing rubber and the double-walled cylinder absorbed the vibration very well.

Correlation between Electrostatic Field Strength and Electrical Charge of Particles Figure 7 shows the relationship between electrostatic field strength and the electrical charge of the particles using different kinds of powdered materials. As can be seen from the figure, a good correlation was obtained between electrostatic field strength and electri-

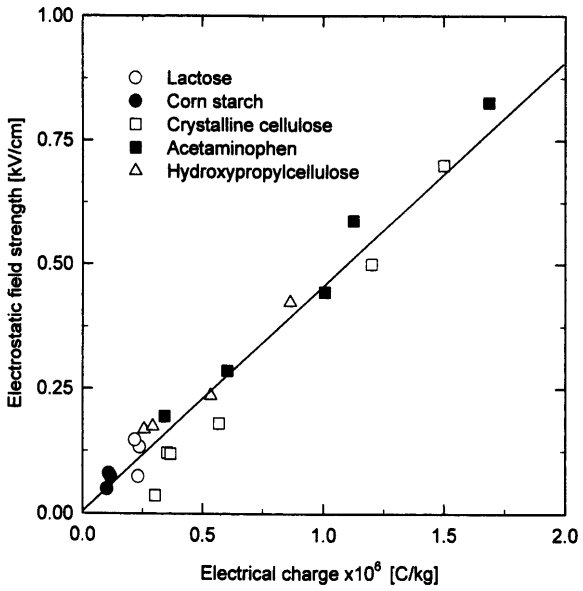

Fig. 7. Relationship between Electrostatic Field Strength and Electrical Charge of Particles

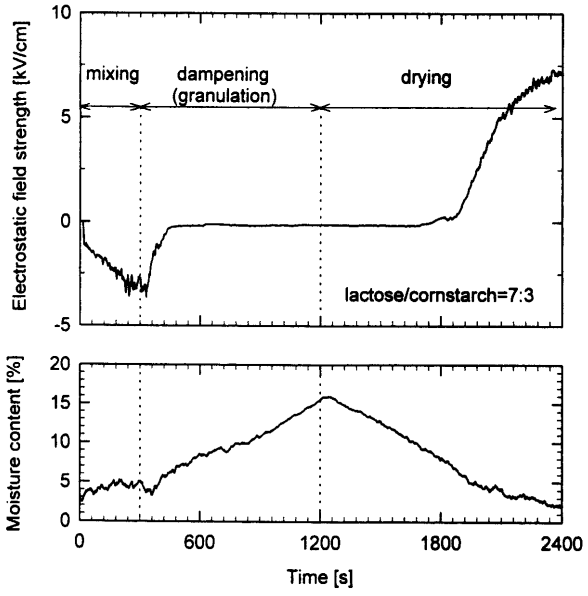

Fig. 8. Electrostatic Field Strength of Lactose and Corn Starch Mixture during Fluidized Bed Mixing, Granulation and Drying Processes

cal charge for various kinds of powdered materials. These results implied that the electrostatic field was induced by the electrical charge of powder, and there existed an obvious quantitative relationship between both quantities. Therefore, measuring the electrostatic field strength meant indirect measurement of the particle electrical charge of powder.

As a result, it could thus be said that the electrostatic characteristics could be monitored continuously by using the system developed. Since this system requires no distance measurement, it is expected to be able to monitor the electrostatic characteristics of charged particles in powder handling processes in which the distance measurement is impossible.

Application of This System to Fluidized Bed Process

To confirm the system's validity, the system was actually applied to fluidized bed mixing, granulation and drying.

Figures 8 illustrates the on-line monitoring data of the electrostatic field strength of lactose and corn starch mixture during fluidized bed mixing, granulation and drying processes. For the lactose and corn starch mixture, the electrostatic field strength showed a negative charge at the mixing and at the initial granulation processes, followed by a zero charge during dampening over $W=7\%$. Though the drying process started, it still showed zero charge until the moisture content decreased under $W=3\%$. After that, electrostatic field strength turned to show a positive charge, and the value increased greatly as the drying process advanced. The change in the electrical charge from negative to positive was presumed to reflect a change in particle composition at the granule surface.

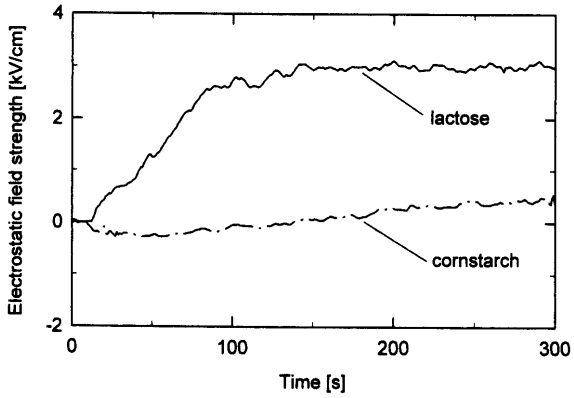

Fig. 9. Electrostatic Characteristics of Lactose and Corn Starch

Figure 9 shows the results of the friction charge between particles and the stainless wall. Here, each particle type (lactose or corn starch) was fluidized for 300 s in the fluidized bed, and the electrostatic field strength was measured continuously. As seen from Fig. 9, lactose particles showed a large positive charge, while corn starch particles indicated only a slight positive charge. This implied that the charge order, the indication of how easy it is to attain an electrical charge, became smaller in the order of, lactose, corn starch and stainless steel. At the initial stage, lactose and corn starch particles were both fluidized and they collided with each other very frequently. When lactose and corn starch collided, lactose showed a positive charge while corn starch, conversely, showed a negative charge. Since the size of the lactose particle was much larger than the corn starch particle, it formed an ordered-mixture,[12] in which most of lactose particle was covered with corn starch particles. Apparently, the electrostatic field strength of the mixture showed a negative charge due to the corn starch coverage.

When the granulation started, the surface was covered with moisture, leading to a sudden decrease in the electrical charge. After that, it showed zero charge. With the progress of drying, the electrostatic field strength showed a positive charge again. This is because the collision between lactose and corn starch decreased due to the granulation (lactose was covered with corn starch), and most of the charge was originated from the collision between the corn starch and the stainless wall. In this case, since corn starch was charged positively and the lactose inside the granules had an originally positive charge, the electrostatic field strength measured showed a positive charge. It should be noted that the sensor has been much improved in terms of detection accuracy and resolution; it could detect the change in polarity of the electrical charge, which was very difficult to obtain *via*

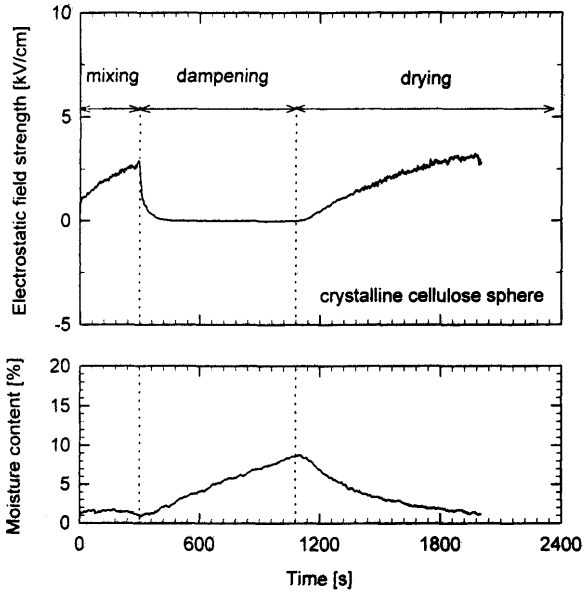

Fig. 10. Electrostatic Field Strength of Crystalline Cellulose Particle during Fluidized Bed Mixing, Granulation and Drying Processes

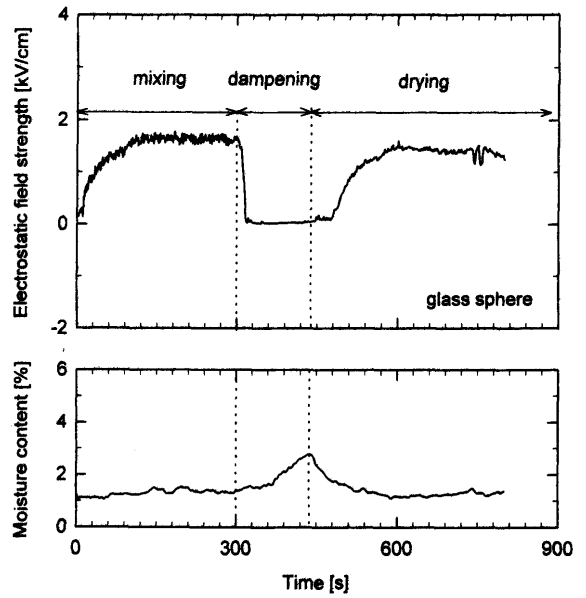

Fig. 11. Electrostatic Field Strength of Glass Sphere during Fluidized Bed Mixing, Granulation and Drying Processes

the previous sensors.[5,6,9]

Figures 10 and 11 describe the behavior of electrostatic field strength during fluidized bed dampening and drying using a crystalline cellulose sphere ($300 \leqq d_p \leqq 500\ \mu m$), and a glass sphere ($350 \leqq d_p \leqq 500\ \mu m$), respectively. Unless the surface coverage changed, the electrostatic field strength showed the same charge for both mixing and drying. It was noted that in the case of crystalline cellulose, the electrostatic field strength began to increase soon after the drying started. The crystalline cellulose particle could absorb water to a great extent. Though it contained much water, surface of the particle was supposed to be pretty dry, like a "sponge", and could accumulate the electrical charge.

In the case of the glass sphere, the electrostatic field strength was greatly affected by moisture content, because it could not absorb water.

Effect of Particle Size on Electrostatic Field Strength

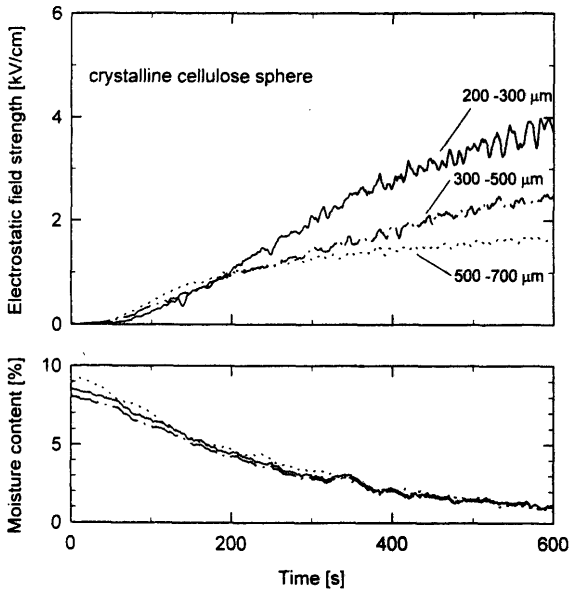

Fig. 12. Effect of Particle Size on Electrostatic Field Strength Measured

Figure 12 shows the effect of particle size on the electrostatic field strength using crystalline cellulose particles of three different sizes. Though each particle showed almost the same behavior in moisture change, the electrostatic field strength varied remarkably with particle size. The smaller particles tended to show larger strength. It was suggested that the interfacial surface area should be increased with a decrease in particle size. Since an electrical charge should occur due to the friction between particle–particle, particle–wall and particle–air, a large interfacial area was effective in generating the electrical charge.

Conclusion

The development of an electrostatic field detecting system comprised of an electrostatic field sensor, a signal conditioning system and an air purge unit was completed. The new sensor tolerated severe vibration, high purge air flow and particle sticking.

This electrostatic field detecting system showed good linearity between electrostatic field strength and the electric charge of particles for various kinds of powdered materials, proving that electrostatic field strength can be used to evaluate the electrostatic characteristics of charged particles. It was confirmed that the electrostatic characteristics could be well monitored in fluidized bed mixing, granulation and drying processes. The mechanism of particle charge was analyzed using different kinds of particles. The effect of particle size on the electrostatic field strength was also investigated. It is expected that this system can be applied to any other powder handling processes to detect the electrostatic characteristics of charged particles.

References

1) Asano K., Jones T. B., Matsubara Y., Proc. of Second IUPAC Workshop on Safety in Chemical Production Processing, Yokohama, September 1993, pp. 1—21.
2) Kodama T., Proc. of the Institute of Electrostatics Jpn., Okayama, October 1995, pp. 2—29.
3) Murasaki N., Masui M., Terada T., *J. Soc. Powder Technol., Jpn.*, **6**, 25—30 (1969).
4) Takeuchi M., *Powder Sci. Eng.*, **28**, 35—45 (1996).
5) Tabata Y., Yagi S., Sakamoto H., Japan. Patent Laid-Open. Patent Pub-

lication No. Heisei 7-1291, 1995.
6) Kodama T., Tabata Y., Nishimura K., Yagi S., Proc. of 1995 Annual Meeting of the Institute of Electrostatics Jpn., Okayama, October 1995, pp. 221—224.
7) Tada Y., Tomizawa Y., Ooi T., Proc. of 1990 Annual Meeting of the Institute of Electrostatics Jpn., Tokyo, October 1990, pp. 149—152.
8) Yamada H., Kobayashi T., Proc. of the Institute of Electrostatics Japan, Beppu, October 1986, pp. 213—216.
9) Watano S., Itoh Y., Suzuki T., Miyanami K., *J. Soc. Powder Technol., Jpn.*, **34**, 778—784, 1997.
10) Watano S., Miyanami K., *Powder Technol.*, **83**, 55—60 (1995).
11) Watano S., Sato Y., Miyanami K., *J. Chem. Eng. Jpn.*, **28**, 282—287 (1995).
12) Watano S., Morikawa T., Mianami K., *J. Chem. Eng. Jpn.*, **28**, 171—178 (1995).